associated with prognosis and the recurrence. In this study, we evaluated CTCs in patients with gastric cancer and explored the clinical impact of CTCs using the CellSearch system.

MATERIALS AND METHODS

Gastric Cancer Cell Line

To prepare for an examination of the CellSearch system, we used the KATO III gastric cancer cell line for the analysis. KATO III cells were cultured in RPMI 1640 (Nissui Pharmaceutical Company, Ltd., Tokyo, Japan) supplemented with 10% fetal calf serum (Mitsubishi Kasei, Tokyo, Japan), 100 U/mL penicillin, and 100 U/mL streptomycin. Cancer cells were grown at 37°C in a humidified atmosphere containing 5% CO_2, as previously described.

Clinical Study Design

Patients with gastric cancer who received treatment at 2 medical centers (Kagoshima University Hospital and Jiaikai Imamura Hospital, Kagoshima, Japan) were analyzed using prospectively collected data. Informed consent was obtained from all patients in accordance with the ethical standards of the Committee on Human Experimentation of Kagoshima University Hospital and Jiaikai Imamura Hospital. We evaluated the usefulness of measuring CTC levels with regard to the overall survival of patients with gastric cancer. In total, 265 consecutive patients with gastric cancer were enrolled between February 2005 and December 2012 at 2 medical centers. Two hundred twenty-eight patients from Kagoshima University Hospital and 37 patients from Jiaikai Imamura Hospital were registered on the study. Fourteen patients were excluded from the analysis, including 12 patients who had another cancer, such as esophageal, colorectal, or prostate cancer, and 2 patients who refused the treatment for gastric cancer. The patients were divided into 2 groups; those who underwent gastrectomy (the resection group; N = 148) and those who did not undergo gastrectomy (the nonresectable group; N = 103) (Fig. 1). Patients in the resection group underwent gastrectomy with standard lymphadenectomy. Patients who had received any preoperative radiotherapy or chemotherapy were excluded from this study. Peripheral blood samples were collected before gastrectomy. Clinical stage was assigned according to the TNM classification.[14]

Patients in the nonresectable group did not undergo surgery because of the presence of distant metastasis or recurrence. Peripheral blood was collected before the beginning of chemotherapy in these patients. In the current study, various chemotherapy regimens were used and mainly included the oral fluoropyrimidine S-1, such as S-1 alone, S-1 plus cisplatin, S-1 plus paclitaxel, and so on.

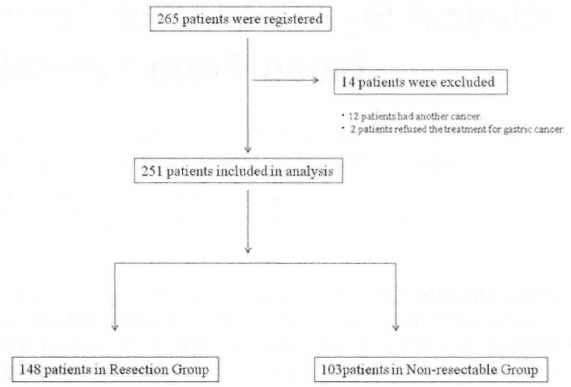

Figure 1. In total, 265 consecutive patients with gastric cancer were enrolled in the study. Fourteen patients were excluded from the analysis: 12 patients had another cancer, and 2 patients refused the treatment for gastric cancer. There were 148 patients with gastric cancer in the resection group and 103 patients who did not undergo gastrectomy in the nonresectable group.

All patients in the resection group were followed after discharge by physical examinations, routine blood tests, serum tumor marker tests (carcinoembryonic antigen [CEA] and cancer antigen 19-9 [CA 19-9]), and computed tomography scans every 3 to 6 months. Follow-up data after discharge were obtained for all patients, and the median follow-up was 31.6 months (range, 4-72 months). In the nonresectable group, patients were evaluated for chemotherapy every 2 to 3 months until death.

Isolation and Enumeration of Circulating Tumor Cells

Ten-milliliter blood samples were drawn into CellSave Preservative Tubes (Veridex, LLC). The samples were maintained at room temperature and processed within 72 hours after collection. All evaluations were performed by technical assistants without knowledge of the clinical status of the patients. The CellSearch system was used to isolate and enumerate CTCs using 7.5 mL of the 10-mL samples. CellSearch is a semiautomated system for the preparation of a sample and is used with the CellSearch Epithelial Cell Kit. The procedure enriches the sample for cells that express epithelial cell adhesion molecule (EpCAM) with antibody-coated magnetic beads, and it labels the nucleus with the fluorescent nucleic acid dye 4,2-diamidino-2-phenylidole dihydrochloride (DAPI).

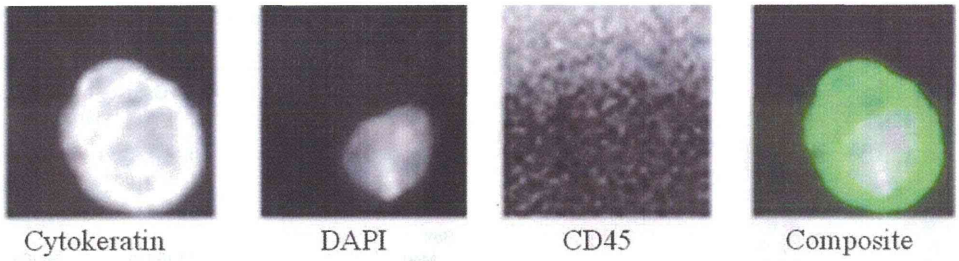

Figure 2. Circulating tumor cells were defined as nucleated cells that lacked allophycocyan (CD45) and expressed cytokeratin. DAPI indicates 4,2-diamidino-2-phenylidole dihydrochloride.

Fluorescently labeled monoclonal antibodies specific for leukocytes (CD45 allophycocyan) and epithelial cells (cytokeratin 8, cytokeratin 19, and 19-phycoerythrin) are used to distinguish epithelial cells from leukocytes. We identified and enumerated CTCs using the Celltracks analyzer II (Veridex, LLC), a semiautomated, fluorescence-based microscopy system that permits the computer-generated reconstruction of cellular images. CTCs were defined as nucleated cells that lacked CD45 and expressed cytokeratin (Fig. 2). Criteria used in the CellSearch system to define a tumor cell have been described previously. The results are expressed as the number of cells per 7.5 mL of whole blood.

Peripheral blood samples for use as a control group were obtained from 15 healthy volunteers who consented to participate. No volunteers had any illness or past history of cancer.

A spiking study was conducted to investigate the detectable limit of the CellSearch system. Therefore, the sensitivity and linearity of the CellSerach system was assessed by spiking a series of 10-fold serial dilutions of KATO III cells (10^2, 50, 10^1, 5, 10^0, and 0 cells) into whole blood from a normal healthy volunteer who did not have any cancer. This in vitro experiment was repeated 3 times for each series.

Statistical Analysis

The chi-square test and the Fisher exact test were used to compare the status of CTCs with categorical clinicopathologic factors. The Kaplan-Meier method was used for survival analysis, and the differences in survival were examined using the log-rank test. Prognostic factors were assessed in univariate and multivariate analyses using Cox proportional hazards regression models. All statistical calculations were performed using SAS statistical software (SAS Institute, Inc., Cary, NC). A P value $< .05$ was considered statistically significant.

RESULTS

Patient Characteristics

The 170 men and 81 women in the cohort ranged in age from 28 to 87 years (mean age, 64.4 years). Sixty-four percent of all patients remained alive at the time of this analysis.

In the resection group, 82 patients underwent distal gastrectomy, 13 patients underwent proximal gastrectomy, and 53 patients underwent total gastrectomy. The final pathologic findings indicated that all patients with disease greater than stage II had oral S-1 recommended as adjuvant chemotherapy for 1 year after surgery. Seventy-four patients (88.1%) were able to tolerate S-1; however, 10 patients (11.9%) were not able to tolerate S-1 because of anorexia and leucopenia. Twenty-six patients (17.6%) in the resection group had developed recurrent disease at the time of this analysis. These patients relapsed an average of 14.9 months after surgery.

In the nonresectable group, 72 patients had primary tumors of the stomach and distant metastasis, and 31 patients had recurrent distant metastasis after gastrectomy. Sixty-one patients had peritoneal dissemination, and 24 patients had para-aortic lymph node or Virchow lymph node swelling. Hematogenous distant metastases were identified in 24 patients. All patients in the nonresectable group received treatment with chemotherapy. The chemotherapy for gastric cancer consisted of S-1 plus cisplatin in 51 patients and S-1 plus paclitaxel in 52 patients.

CTCs were not identified in any samples from the healthy volunteers. In this study, the presence of ≥ 0 CTCs per 7.5 mL of blood was considered a positive result.

Circulating Tumor Cells and Clinical Correlation

Seventy-eight of 251 patients had CTCs detected. CTCs were detected in 16 patients (11.3%) from the resection

Figure 3. Circulating tumor cells (CTCs) were detected in 16 patients (10.8%) from the resection group and in 62 patients (60.2%) from the nonresectable group. The average number of CTCs was 3.5 in the resection group and 109.3 in the nonresectable group. CTCs were not observed in any samples from healthy volunteers.

group and in 62 patients (60.2%) from the nonresectable group. There was a significant difference in the positive rate between the 2 groups ($P < .0001$). Among those who had CTCs detected, the average count was 3.5 CTCs in patients from the resection group and 109.3 CTCs in patients from the nonresectable group (Fig. 3). The overall survival rate for all patients was significantly lower among those who had CTCs detected than among those who did not ($P < .0001$) (Fig. 4A).

In the resection group, CTCs were detected in 1 patient (1.6%) with a T1 tumor, in 2 patients (11.1%) with T2 tumors, in 6 patients (16.2%) with T3 tumors, and in 7 patients (23.3%) with T4 tumors. Clinicopathologic findings from the resection group are provided in Table 1. CTCs in patients who underwent gastrectomy were significantly correlated with the depth of tumor invasion, lymph node metastasis, distant metastasis, disease stage, vessel invasion, and lymphatic invasion. Although serum tumor markers like CEA and CA 19-9 were added to our analysis to be compared with CTCs, there was no significant correlation between CTCs and serum tumor markers.

Among 132 patients without CTCs, 14 patients (10.6%) had a recurrence after surgery. Eight patients had peritoneal dissemination, and 3 patients had hematogenous recurrences. Conversely, 12 of 16 patients (75%) with CTCs had a recurrence after surgery. The patients who had CTCs detected had a significantly higher relapse rate compared with patients who did not have CTCs detected ($P < .0001$). Two patients without recurrence on diagnostic imaging had transient elevation of serum CEA.

TABLE 1. Characteristics of Patients in the Resection Group

Variable	CTCs: No. of Patients (%)		
	Positive, n = 16	Negative, n = 132	*P*
Sex			
Men	11 (68.8)	88 (66.7)	.867
Women	5 (31.2)	44 (33.3)	
Age, y			
<70	8 (50)	83 (62.9)	.317
>70	8 (50)	49 (37.1)	
Tumor classification			
T1	1 (6.3)	62 (47)	.009
T2	2 (12.5)	16 (12.1)	
T3	6 (37.5)	31 (23.5)	
T4	7 (43.8)	23 (17.4)	
Lymph node classification			
N0	2 (12.5)	80 (60.6)	< .0001
N1	0 (0)	19 (14.4)	
N2	1 (6.3)	17 (12.9)	
N3	13 (81.3)	16 (12.1)	
Distant metastasis			
Yes	3 (18.8)	5 (3.8)	.012
No	13 (81.2)	127 (96.2)	
Stage			
I	1 (6.3)	63 (47.7)	.0002
II	1 (6.3)	25 (18.9)	
III	11 (68.8)	39 (29.5)	
IV	3 (18.8)	5 (3.8)	
Lymphatic invasion			
0	1 (6.3)	71 (53.8)	.0003
1	15 (93.7)	61 (46.2)	
Vessel invasion			
0	3 (18.8)	73 (55.3)	.006
1	13 (81.2)	59 (44.7)	
Histologic type			
Differentiated	3 (18.8)	39 (29.5)	0.365
Undifferentiated	13 (81.2)	93 (70.5)	—

Abbreviations: CTCs, circulating tumor cells.

Peritoneal dissemination was the most common pattern of recurrence, and 5 patients had hematogenous recurrences (Table 2). There were no significant differences in the recurrence pattern between patients with and without CTCs. However, all patients who had CTCs detected, at the least, had either peritoneal dissemination or hematogenous distant metastases. The sensitivity and specificity for predicting recurrences were 46.2% and 96.7%, respectively.

When we analyzed relapse-free survival according to whether patients were positive for CTCs, relapse-free survival in patients who were positive for CTCs was significantly lower than in those who were negative ($P < .0001$) (Fig. 4B). Furthermore, the 5-year survival rate also was significantly lower in patients with CTCs than in those without CTCs ($P < .0001$) (Fig. 4C). Multivariate analysis demonstrated that the presence of CTCs was an

independent prognostic factor (Table 3). Factors that we included in this analysis were CTCs, tumor classification, lymph node classification, lymphatic invasion, and vessel invasion, all of which were considered to be significant characteristics in these patients. It is noteworthy that positive expression of CTCs in peripheral blood was identified as an independent factor for overall survival in patients with gastric cancer (hazard ratio, 1.73; 95% confidence interval, 1.08-2.77; $P = .024$).

All patients of the nonresectable group received chemotherapy. There was no significant correlation between the presence of CTCs and nonresectable factors (Table 4). In these 103 patients, the presence of CTCs was correlated with a lower survival rate ($P = .0044$) (Fig. 4D). The median survival was 248 days in patients with CTCs and 582 days in patients without CTCs.

TABLE 2. Recurrence Pattern of 16 Patients With Circulating Tumor Cells in the Resection Group

Postgastrectomy	No. of Patients (%)
Recurrence pattern	12 (75)
Peritoneal dissemination	9 (56.3)
Liver metastasis	2 (12.5)
Bone metastasis	2 (12.5)
Adrenal gland metastasis	1 (6.3)
Lymph node metastasis	1 (6.3)
No recurrence	4 (25)

Sensitivity of the CellSearch System With Cell Line

KATO III cells were used for the analysis of sensitivity and linearity of the CellSearch system. Representative results from the expected number of KATO III cells spiked into healthy donor samples plotted against the actual number of KATO III cells observed in the samples are illustrated in Figure 5. Regression analysis of the

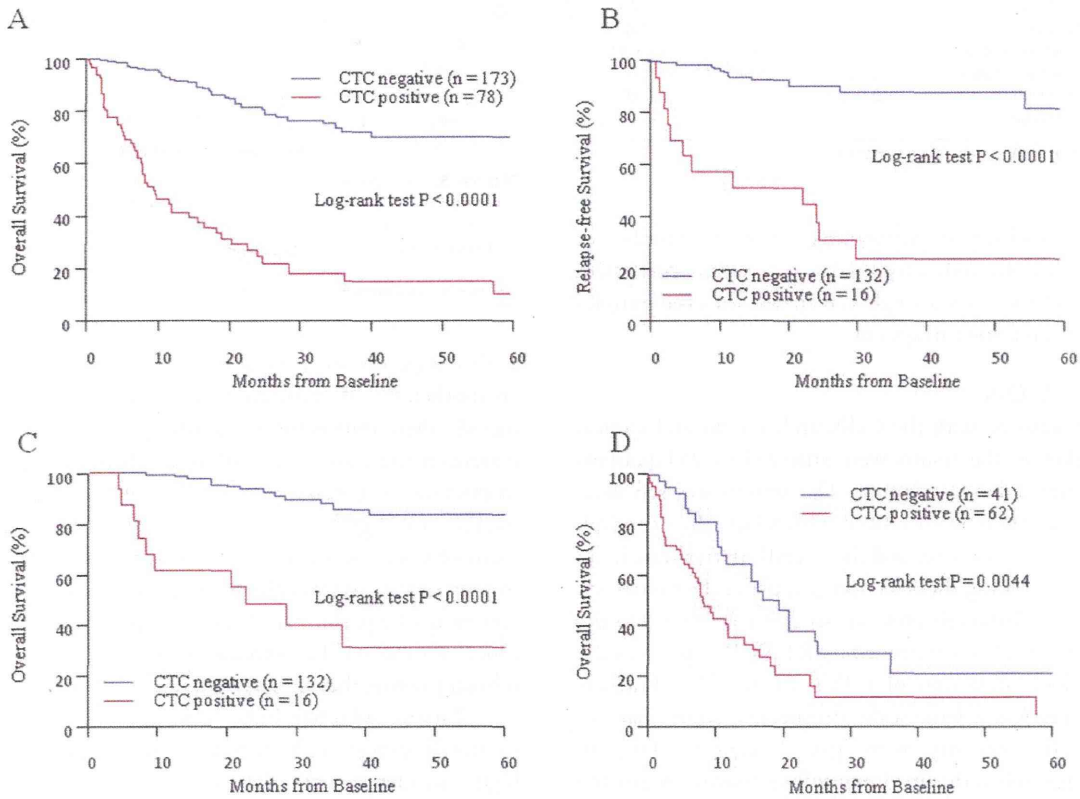

Figure 4. (A) Circulating tumor cells (CTCs) were detected in 78 of 251 patients. The 5-year survival rate was significantly lower in patients with CTCs than in those without CTCs ($P < .0001$). (B) In the resection group, the relapse-free survival rate was significantly lower in patients with CTCs than in those without CTCs ($P < .0001$). (C) The overall survival rate also was significantly lower in patients with CTCs than in those without CTCs ($P < .0001$). (D) In the nonresectable group, the overall survival rate was significantly lower in patients with CTCs than in those without CTCs ($P = .0044$). The median survival was 248 days in patients with CTCs and 582 days in patients without CTCs.

TABLE 3. Univariate and Multivariate Analysis in the Resection Group

	Univariate Analysis		Multivariate Analysis	
Independent Factor	HR (95% CI)	*P*	HR (95% CI)	*P*
Depth of tumor invasion	2.33 (1.56-3.69)	< .0001	1.45 (0.82-2.69)	.204
Lymph node metastasis	2.60 (1.80-4.04)	< .0001	1.53 (0.91-2.69)	.114
Distant metastasis	3.85 (1.11-10.28)	.035	0.87 (0.23-2.59)	.807
Lymphatic invasion	10.41 (3.05-65.08)	< .0001	1.73 (0.33-13.90)	.541
Vessel invasion	7.53 (2.58-31.99)	< .0001	1.62 (0.39-9.07)	.526
CTCs	2.77 (1.81-4.18)	< .0001	1.73 (1.08-2.77)	.024

Abbreviations: CI, confidence interval; CTCs, circulating tumor cells; HR, hazard ratio.

TABLE 4. Nonresectable Factors in the Nonresectable Group

	No. With CTCs		
Nonresectable Factor	Positive	Negative	Incidence of CTCs, %
Liver metastasis	9	7	56.3
Lung metastasis	0	2	0
Bone metastasis	4	1	80
Brain metastasis	2	0	100
Peritoneal dissemination	40	23	63.5
Lymph node metastasis	12	12	50
Direct invasion to peripheral organs	2	3	40

Abbreviations: CTCs, circulating tumor cells.

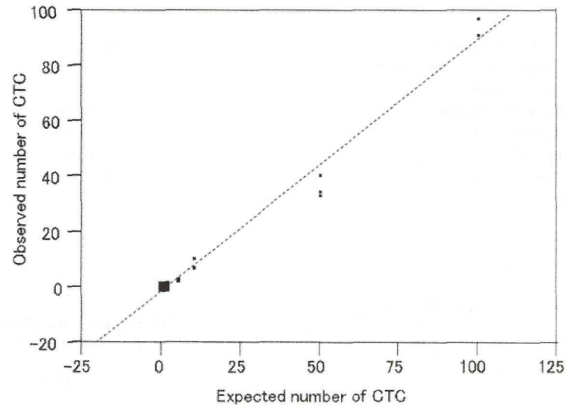

Figure 5. Regression analysis of the number of observed tumor cells versus the number of expected tumor cells produced a correlation coefficient (R^2) of 0.985. Even a single cell spiked into the samples was detected using this system.

number of observed tumor cells versus the number of expected tumor cells produced a correlation coefficient (R^2) of 0.985. Even a single cell spiked into the samples was detected using this system.

DISCUSSION

CTCs measured with the CellSearch system and clinical correlation of the results were analyzed in 251 patients with gastric adenocarcinoma. The system was sensitive, and the results were correlated with relapse-free survival, the 5-year survival rate, and the overall survival rate in all patients, including the resection group and the nonresectable group. Although previous studies have reported the presence of CTCs determined by RT-PCR, reports of the morphologic detection of CTCs are few.[15-19] Furthermore, ours was a large-scale, prospective study that enrolled 265 patients with gastric cancer. To our knowledge, this is the first longitudinal analysis evaluating CTCs using the CellSearch system in such patients.

In Japan, almost all patients who have stage II or III tumors after undergoing gastrectomy receive adjuvant chemotherapy in the form of oral S-1 according to data from the Adjuvant Chemotherapy Trial of TS-1 for Gastric Cancer (ACTS-GC).[20] However, ≥60% of patients at this stage do not have a recurrence without adjuvant chemotherapy. If recurrence after surgery can be predicted, then information regarding CTCs could help patients avoid unnecessary adjuvant chemotherapy. This distinction is necessary to determine whether or not patients are eligible for curative resection. The measurement of CTCs in gastric cancer will be useful for determining treatment strategies if more accurate staging of the patient can be performed. Moreover, patients with gastric cancer who have CTCs should receive neoadjuvant chemotherapy before they undergo surgery.

Patients who had breast cancer, prostate cancer, or colorectal cancer with hematogenous metastasis had a high incidence of CTCs according to several reports.[12,13,21] However, no significant correlation between positive CTCs and hematogenous distant metastasis in gastric cancer has been demonstrated. In the current study, peritoneal dissemination was the most frequently observed pattern of recurrence. The detection of CTCs may be a useful diagnostic tool for predicting

peritoneal dissemination, which is difficult to detect on imaging studies, such as computed tomography, ultrasonography, and positron emission tomography.

The prognosis of patients in our nonresectable group also differed significantly according to the presence of CTCs. Some authors have reported that response to chemotherapy can be evaluated in several cancers with distant metastasis. Monitoring the number of CTCs may be more useful for evaluating chemotherapy.[22,23] It is an advantage that the measurement of CTCs using the CellSearch system is available at any time and is easily and noninvasively performed. An increase in the number of CTCs should lead to a change in chemotherapy regimen.

The CellSearch system is based on the enumeration of epithelial cells, which are separated from the blood by EpCAM antibody-coated magnetic beads and identified with the use of fluorescently labeled antibodies against cytokeratin and with a fluorescent nuclear stain. In the detection of CTCs by molecular techniques there is always the question of whether the result could be a false-positive. Although Sensitivity of RT-PCR is very high for CTCs identification, it is impossible to visually confirm cancer cells. Conversely, with the Cell Search system (Janssen Diagnostics, LLC, Raritan, NJ), the false-positive rate is extremely low, because it is possible to morphologically confirm the presence of cells. Conversely, some cases might be missed (false-negative) because some of the CTCs may not express these epithelial markers and may be undetectable by the CellSearch system.[24]

Most reports concerning the prognosis for patients with breast cancer and prostate cancer have used a cutoff of $\geq$5 CTCs to determine a positive test.[12,13] Conversely, some reports of other cancers use different cutoff values.[25] The question remains regarding the significance of the presence of a single CTC. For patients with gastric cancer who have undergone curative resection, this single cell may be consequential. Our criteria defined $\geq$1 CTC as a positive test. It is important to note that CTCs were not detected in healthy volunteers in our series. In fact, several patients in our cohort who had only 1 CTC relapsed, and the presence of any CTCs in peripheral blood was considered an independent prognostic factor for determining the overall survival of patients who underwent gastrectomy. It may become possible to more accurately estimate the prognosis for these patients if the presence of CTCs is added to the staging factors. In this study, many patients who were positive for CTCs had a recurrence, and several patients who did not have a recurrence had received chemotherapy because of up-regulated serum tumor marker levels during follow-up. The detection of CTCs is useful for predicting recurrence and prognosis. We conclude that the evaluation of CTCs in peripheral blood may be a useful tool for predicting tumor progression, prognosis, and the effect of chemotherapy in patients with gastric cancer.

FUNDING SUPPORT

This work was supported in part by a grant-in-aid (no. 22501032) for scientific research from the Ministry of Education, Science, Sports, and Culture of Japan.

CONFLICT OF INTEREST DISCLOSURES

The authors made no disclosures.

REFERENCES

1. Yeh KH, Chen YC, Yeh SH, Chen CP, Lin JT, Cheng AL. Detection of circulating cancer cells by nested reverse transcription-polymerase chain reaction of cytokeratin-19 (K19)—possible clinical significance in advanced gastric cancer. *Anticancer Res.* 1998;18:1283-1286.
2. Noh YH, Kim JA, Lim GR, et al. Detection of circulating tumor cells in patients with gastrointestinal tract cancer using RT-PCR and its clinical implications. *Exp Mol Med.* 2001;33:8-14.
3. Vogel I, Kalthoff H. Disseminated tumour cells. Their detection and significance for prognosis of gastrointestinal and pancreatic carcinomas. *Virchows Arch.* 2001;439:109-117.
4. Ghossein RA, Bhattacharya S, Rosai J. Molecular detection of micrometastases and circulating tumor cells in solid tumors. *Clin Cancer Res.* 1999;5:1950-1960.
5. Nakashima S, Natsugoe S, Matsumoto M, et al. Clinical significance of circulating tumor cells in blood by molecular detection and tumor markers in esophageal cancer. *Surgery.* 2003;133:162-169.
6. Mimori K, Fukagawa T, Kosaka Y, et al. A large-scale study of MT1-MMP as a marker for isolated tumor cells in peripheral blood and bone marrow in gastric cancer cases. *Ann Surg Oncol.* 2008;15:2934-2942.
7. Bertazza L, Mocellin S, Marchet A, et al. Survivin gene levels in the peripheral blood of patients with gastric cancer independently predict survival [serial online]. *J Transl Med.* 2009;7:111.
8. Wu CH, Lin SR, Hsieh JS, et al. Molecular detection of disseminated tumor cells in the peripheral blood of patients with gastric cancer: evaluation of their prognostic significance. *Dis Markers.* 2006;22:103-109.
9. Mimori K, Fukagawa T, Kosaka Y, et al. Hematogenous metastasis in gastric cancer requires isolated tumor cells and expression of vascular endothelial growth factor receptor-1. *Clin Cancer Res.* 2008;14:2609-2616.
10. Koga T, Tokunaga E, Sumiyoshi Y, et al. Detection of circulating gastric cancer cells in peripheral blood using real time quantitative RT-PCR. *Hepatogastroenterology.* 2008;55:1131-1135.
11. Arigami T, Uenosono Y, Ishigami S, Hagihara T, Haraguchi N, Natsugoe S. Clinical significance of the B7-H4 coregulatory molecule as a novel prognostic marker in gastric cancer. *World J Surg.* 2011;35:2051-2057.
12. Cristofanilli M, Budd GT, Ellis MJ, et al. Circulating tumor cells, disease progression, and survival in metastatic breast cancer. *N Engl J Med.* 2004;351:781-791.
13. Leversha MA, Han J, Asgari Z, et al. Fluorescence in situ hybridization analysis of circulating tumor cells in metastatic prostate cancer. *Clin Cancer Res.* 2009;15:2091-2097.
14. Sobin LH, Gospodarowicz MK, Wittekind C, eds. TNM Classification of Malignant Tumours. 7th ed. Oxford, United Kingdom: Wiley-Blackwell; 2010.

15. Nishida S, Kitamura K, Ichikawa D, Koike H, Tani N, Yamagishi H. Molecular detection of disseminated cancer cells in the peripheral blood of patients with gastric cancer. *Anticancer Res.* 2000;20:2155-2159.
16. Ikeguchi M, Ohro S, Maeda Y, et al. Detection of cancer cells in the peripheral blood of gastric cancer patients. *Int J Mol Med.* 2003; 11:217-221.
17. Miyazono F, Natsugoe S, Takao S, et al. Surgical maneuvers enhance molecular detection of circulating tumor cells during gastric cancer surgery. *Ann Surg.* 2001;233:189-194.
18. Arigami T, Uenosono Y, Hirata M, Yanagita S, Ishigami S, Natsugoe S. B7-H3 expression in gastric cancer: a novel molecular blood marker for detecting circulating tumor cells. *Cancer Sci.* 2011; 102:1019-1024.
19. Saad AA, Awed NM, Abd Elkerim NN, et al. Prognostic significance of E-cadherin expression and peripheral blood micrometastasis in gastric carcinoma patients. *Ann Surg. Oncol.* 2010;17:3059-3067.
20. Sakuramoto S, Sasako M, Yamaguchi T, et al. Adjuvant chemotherapy for gastric cancer with S-1, an oral fluoropyrimidine. *N Engl J Med.* 2007;357:1810-1820.
21. Rahbari NN, Bork U, Kircher A, et al. Compartmental differences of circulating tumor cells in colorectal cancer. *Ann Surg Oncol.* 2012;19:2195-2202.
22. Budd GT, Cristofanilli M, Ellis MJ, et al. Circulating tumor cells versus imaging—predicting overall survival in metastatic breast cancer. *Clin Cancer Res.* 2006;12:6403-6409.
23. Nakamura S, Yagata H, Ohno S, et al. Multi-center study evaluating circulating tumor cells as a surrogate for response to treatment and overall survival in metastatic breast cancer. *Breast Cancer.* 2010;17:199-204.
24. Sakakura C, Hagiwara A, Nakanishi M, et al. Differential gene expression profiles of gastric cancer cells established from primary tumour and malignant ascites. *Br J Cancer.* 2002;87:1153-1161.
25. Hiraiwa K, Takeuchi H, Hasegawa H, et al. Clinical significance of circulating tumor cells in blood from patients with gastrointestinal cancers. *Ann Surg. Oncol.* 2008;15:3092-3100.

CellBio, 2013, 2, 179-185
Published Online December 2013 (http://www.scirp.org/journal/cellbio)
http://dx.doi.org/10.4236/cellbio.2013.24020

Scientific Research

Immunohistochemical Analysis of the Acid Secretion Potency in Gastric Parietal Cells

Rie Irie-Maezono[1], Shinichiro Tsuyama[2]
[1]Department of Gene Therapy and Regenerative Medicine, Kagoshima University, Graduate School of Medical and Dental Sciences, Kagoshima, Japan
[2]Laboratory for Neuroanatomy, Kagoshima University, Graduate School of Medical and Dental Sciences, Kagoshima, Japan
Email: maezono@m.kufm.kagoshima-u.ac.jp

Received July 31, 2013; revised August 31, 2013; accepted September 7, 2013

ABSTRACT

Gastric parietal cells are important in acid secretion, but it is unclear which cells throughout the gastric gland have the highest secretion potency. Here, we used immunohistochemical methods with anti-H^+, K^+-ATPase, phosphoryl ezrin and CD44 antibodies to study the distribution of gastric acid secretion activity. Stomach tissues from freely fed and starved rats were cryofixed for light microscopy or fixed by high-pressure freezing for electron microscopy. Parietal cells from freely fed animals corresponded to the active secretion phase and to the inactive resting phase from starved rats. Anti-H^+, K^+-ATPase and anti-phosphoryl ezrin labeling were observed on the membrane of the intracellular canaliculi and the tubulovesicle from freely fed rats, while cells from starved animals showed weak labeling with anti-phosphoryl ezrin antibody staining. Morphometrical analysis at the electron microscopic level was performed on active and inactive acid secretory phases between the upper and base regions of the gland. H^+, K^+-ATPase and CD44 were distributed on both sites of the microvillous and tubulovesicle membrane in the same cells, but phosphoryl ezrin localized predominantly on the microvillous membrane in active cells of the glandular neck and upper base. Therefore, the highest secreting potency appeared to be in cells of the glandular neck and upper base.

Keywords: Gastric Parietal Cells; Secretory Potency; Phosphoryl Ezrin; Histochemical Morphometry

1. Introduction

Gastric parietal cells play a major role in acid secretion and are widely distributed from the pit to the base of rat gastric glands. They show characteristic aspects of intracellular canaliculi (IC) with numerous microvilli and tubulovesicles (TV) in the cytoplasm, which are thought to be interconvertable structures. Although the conversion mechanism for these structures is unclear, various hypothesizes have been proposed. During the active acid-secreting phase of parietal cells, the IC is markedly expanded, but the cells undergo a morphological transformation during their inactive resting phase when the IC reduces in width and the TV mass increases [1,2]. The secretion activity alternates according to the physiological phases of feeding or starving.

Proton potassium ATPase (H^+, K^+-ATPase; "the proton pump") is an important enzyme for gastric acid secretion and exists as an integral membrane-protein along the IC and TV throughout the parietal cell membrane. We previously used high-pressure freezing followed by freeze-substitution to investigate the histochemistry of gastric gland cells and the ultrastructural alterations that occur in both fed and starved phases [3,4]. Cryofixation using rapid freezing (especially high pressure rapid freezing for capable freezing depth) is believed to be superior to conventional chemical fixation with regard to morphological preservation and retention of soluble components. Using antibodies against the proton potassium ATPase α- and β-subunits, we also showed that the enzyme localized on both IC and TV membranes in almost all parietal cells throughout the length of the gland [3-5].

Parietal cells contain more actin than other glandular cells. Transformation between IC and TV occurs with redistribution of actin in the cell. Filamentous actins are anchored to the plasma membrane via phosphoryl ezrin,

and most actin molecules are thought to form a globular structure in the inactive resting state, which molecules polymerize rapidly to form a filamentous structure upon active acid secretion [2,6-11]. Ezrin is a member of the ERM (ezrin/radixin/moesin) family of proteins that is implicated in linking functional activities of the plasma membrane to the actin cytoskeleton. In addition, actin binds to intramembranous CD44 via phosphoryl ezrin in the plasma membrane [12-14]. It has previously been suggested that the above-mentioned morphological changes are induced and triggered by this cytoskeletal reorganization of β-actin [15-17].

The purpose of the present study was to investigate which parietal cells are more active than others in terms of acid secretion, based on the distribution of phosphoryl ezrin and CD44 throughout the gland using immunohistochemical techniques.

2. Materials and Methods

2.1. Tissue Preparation

Ten male Wistar rats were used in the experiments and divided into two groups of five animals each. One group was fed freely and the other was starved for 48 h with free access to water. The rats were anesthetized with an intraperitoneal injection of sodium pentobarbital, and the pH of the luminal gastric juice was determined. The stomach tissues were cut into small pieces and cryofixed using a rapid freezing device (RF-6, Eiko, Japan) using liquid propane for cryofixing and liquid nitrogen for light microscopy. The specimens were then freeze-substituted with acetone containing 0.2% glutaraldehyde at −79°C for 72 h and embedded in paraffin [17].

For electron microscopy, the specimens underwent high-pressure freezing under a 21×10^5 hPa atmosphere (HPM 010, BAL-TEC, Liechtenstein). The frozen specimens were freeze-substituted with acetone containing 1% osmium tetroxide or 0.2% glutaraldehyde at −79°C for 72 h and were embedded in Epon812 or Lowicryl K4M resin, respectively [3].

2.2. Primary and Secondary Antibodies

A rabbit antibody against the H^+, K^+-ATPase (proton pump) α-subunit (Immunogen; C-terminal synthetic peptide based on the porcine H^+, K^+-ATPase α-subunit sequence) was purchased from Calbiochem-Novabiochem (San Diego, CA). The antibody was used at a dilution of 1:100 in phosphate buffered saline (PBS). A mouse monoclonal antibody against the H^+, K^+-ATPase β-subunit (Immunogen; purified 34-kDa core peptide from deglycosylated hog gastric microsomes) was purchased from Abcam Ltd. (Cambridge, UK) and diluted 1:200 in PBS. A rabbit polyclonal antibody against phosphoryl ezrin (Immunogen: KLH-conjugated, synthetic phosphopeptide corresponding to residues surrounding Thr567 of human ezrin) and an anti-CD44 antibody were purchased from CHEMICON International, Inc. (Temecula, CA). These were used at a dilution of 1: 10 - 20 in PBS. A mouse monoclonal antibody against actin (pan Ab-5; Clone ACTN05) was purchased from LAB VISION Co. (Fremont, CA). This antibody reacts with all six known isoforms of vertebrate actin (MW-42 kD) and also with two highly homologous cytoplasmic actins (β, γ). This antibody was diluted 1: 10 - 80 in PBS. The antibodies were confirmed to show cross-reactivity against the rat. The following were used as secondary antibodies: biotinylated goat anti-mouse immunoglobulin ($F(ab')_2$) or biotinylated swine anti-rabbit immunoglobulin (DAKO Cytomation, Glostrup, Denmark) diluted 1: 100 - 200 in PBS; horseradish peroxidase (HRP)-conjugated streptavidin (DAKO Cytomation) (1:200 in Tris-buffered-saline; TBS); colloidal gold (CG)-conjugated streptavidin (1:1 in PBS) from British BioCell International (Cardiff, UK).

2.3. Immunohistochemical Staining for Light Microscopy

Specimens embedded in paraffin were cut into 4 μm-thick slices with a sliding Jung-model microtome, mounted on silconized glass slides and air-dried. Sections were deparaffinized, rehydrated and immersed in PBS. After blocking endogenous peroxidase activity with 0.3% hydrogen peroxide in methanol, specimens were incubated with primary antibodies against the H^+, K^+-ATPase α- and β-subunits. They were then labeled with biotinylated anti-rabbit or anti-mouse IgG antibodies overnight followed by HRP-conjugated streptavidin for 1 h. Visualization was performed using 3, 3'-diaminobenzidine tetrahydrochloride (DAB; DAKO Cytomation) for 10 min. Finally, sections were rinsed in distilled water, counterstained with Mayer's hematoxylin, dehydrated in a graded ethanol series, cleared in xylene and mounted with Eukitt (O. Kindler, Germany).

2.4. Electron Microscopy

Ultrathin sections from specimens fixed with 1% osmium tetroxide and embedded in epoxy resin were cut with a Reichert Ultracat-N ultramicrotome and stained with uranyl acetate and Reynolds' lead citrate. They were observed using a HITACHI H-7000 electron microscope at an acceleration voltage of 80 kV.

Specimens fixed with 0.2% glutaraldehyde and embedded in Lowicryl K4M resin were stained by the immunogold method (particle size of colloidal gold (CG): 15 nm and 10 nm). Thin sections were incubated with unlabeled-streptavidin (Southern Biotech, Birmingham, AL) for 30 min at room temperature to block endogenous

biotin. Immunogold staining was performed as described previously [4,18]. Briefly, the sections were incubated with anti-H^+, K^+-ATPase α- and β-subunits, anti-phosphoryl ezrin and anti-CD44 antibodies followed by biotinylated anti-rabbit or anti-mouse IgG antibodies and labeled with streptavidin-colloidal gold. Finally, the sections were counterstained with uranyl acetate and Millonig's lead acetate.

2.5. Morphometrical Analysis of Labeling Density with Phosphoryl Ezrin Immunogold Staining

The parietal cell labeling density with the anti-phosphoryl ezrin antibody was analyzed using Image-J NIH software. Thus, the labeling number of gold particles (on IC containing multiple microvilli) was counted on electron microscopic photographs taken at 15,000 × magnification of the neck or base region (n = 20 each) of active phase glands (fed animals) and inactive resting phase glands (starved animals). The labeling density was estimated as the number of gold particles per unit area (μm^2) of IC. For the assessment of the phosphoryl ezrin labeling-density, the results were statistically analyzed by *t*-test using Microsoft Excel software. Statistical comparisons were made between the neck and the base area of the gland, and between active versus inactive glands from starved animals. The differences between sites or feeding/starving were evaluated by *t*-test. $P < 0.01$ or 0.05 was considered significant. The results are expressed as the arithmetic mean ± SE.

3. Results

3.1. Morphological Observation

The average pH in the fed rats was 2.0, compared with 6.4 in the starved rats. We therefore hypothesized that the former corresponds to the active phase and the latter to the inactive resting phase of gastric juice secretion.

The parietal cells showed excellent ultrastructural preservation at the electron microscopic level. The ultrastructure of IC, TV, and other organelles was well preserved for each active and inactive phase of glands when specimens were processed successfully by means of HPF-followed by FS.

3.2. Immunohistochemical Observation with Anti-H^+, K^+-ATPase Antibody

The parietal cells were labeled intensely and clearly by immunohistochemical staining with the H^+, K^+-ATPase anti-α- and -β-subunit antibodies. Cells in the neck and upper base were labeled particularly strongly in active phase animals. Staining was evenly distributed from the deep pit to the glandular base of the cells (**Figures 1(A)** and **(B)**), and the staining pattern was similar between the anti-β-subunit antibody and α-subunit antibody (data not shown). In the active phase, the microvillous membrane and apical cell membrane of the IC were labeled with the anti-α- and -β-H+, K+-ATPase subunit antibodies and with the anti-phosphorylated-ezrin antibody (corresponding to residues surrounding Thr566 and 567), while TV membranes were hardly stained. In the inactive phase, IC microvilli were labeled weakly with this antibody. The anti-CD44 antibody staining pattern was similar to that of anti-α- (and -β-) H^+, K^+-ATPase subunit antibodies in inactive phase animals (**Figures 2, 3(A)** and **(B)**). A regional labeling difference was evident from the neck to the upper base and lower base.

3.3. Morphometric Analysis with Anti-Phosphoryl Ezrin Antibody and Immunogold Labeling

Immunogold staining was performed to examine the intracellular distribution and the labeling density of the

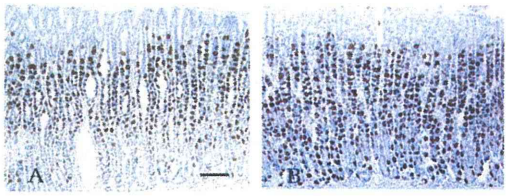

Figure 1. Active phase rat gastric gland immunostained with the anti-H^+, K^+-ATPase α-subunit antibody. (A) Parietal cells throughout the gland are stained strongly. Cells are large and plump and become smaller and more slender as they migrate downwards. Reaction products are thread-like in shape; (B) Inactive resting phase gland with similar staining. Parietal cells scattered throughout the gland are also stained positively and reaction products were observed diffusely in the cytoplasm. Scale bar = 100 μm.

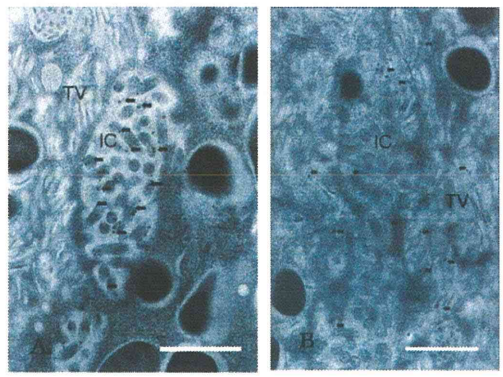

Figure 2. Section of parietal cells stained with immunogold method. (A) Anti-phosphoryl ezrin antibody staining. The IC membrane and its microvilli were stained with anti-phosphoryl ezrin antibody, but little staining was visible on the TV membrane; (B) Anti-CD44 ant-ibody staining. The two organelles (IC and TV) were labeled with this antibody. Scale bar = 1 μm.